HINS SS1 Magnetic Performance Study

Andrés G. Delannoy
Fermi National Accelerator Laboratory
University of Puerto Rico at Mayagüez

***Abstract*—This paper offers an analysis of the performance of the HINS SS1 as recorded by a magnetic measurement Hall probe array. These superconducting solenoids are under development for a R&D project named High Intensity Neutrino Source. The project design demands an especially small stray field due to adjacent RF cavities. The Hall probe array was fitted with small test coils for probe calibration and testing. Each probe's sensitivity was measured at diminishing magnetic fields, and the system's ability to resolve and recover the amplitude of the magnetic field was determined. The system was found to resolve magnetic fields well under 10 μT. These results were reproduced at superconducting temperatures using a different Hall probe excitation method and the stray field found to satisfy the design requirements to first approximation.**

***Index Terms*—Fringe Field, Hall Probe, LabVIEW, Solenoid, Superconductor**

I. INTRODUCTION

THE High Intensity Neutrino Source is a R&D superconducting proton linear accelerator program under development at Fermi National Accelerator Laboratory. The project aims to demonstrate the feasibility of new technology in low-energy, high-intensity, proton linac applications. Its design features superconducting spoke-type accelerator cavities, superconducting solenoids for transverse focusing, and high power RF vector modulators for independent control of multiple cavities powered by a single klystron.

The project may ultimately be a likely replacement of the aging 8 GeV injector complex at Fermilab. This type of a front end would facilitate and support neutrino physics and muon storage/collider experiments. A 60 MeV HINS linac is currently under construction at the Meson Facility.

Collaborations with Argonne National Laboratory and Lawrence Berkeley National Laboratory have provided support in the design and development of spoke-type SRF accelerators and studies of electron cloud issues. Brookhaven National Laboratory has reviewed an 8 GeV H- beam transport line design and offered consultation on H- injection and stripping [9].

The design achieves initial beam acceleration using room temperature Crossbar-H (CH) copper RF cavities, interlaced with superconducting focusing solenoids in their individual cryostat. In the higher energy accelerating sections, the solenoids will be interleaved with Superconducting Spoke Resonator (SSR) cavities and share a single, long cryomodule. Currently, testing is being performed on a pre-production solenoid for the superconducting section of the linac [8].

The studies presented in this paper were focused on the SSR section solenoids. The magnetic measurement equipment was tested to verify its ability to resolve such weak magnetic fields. The stray field at the distance corresponding to the SRF cavity wall was examined to validate the solenoid's design requirements.

II. HINS SS1 DESIGN

The SS1 section solenoid design requires a ~5 T operating field at its center, 30 mm diameter cold bore, around 25% operating current margin, and an integrated field strength of $\mathrm{IS} = \int_{-\infty}^{\infty} \mathrm{B}_z^2 \mathrm{dz} = 300\ \mathrm{T}^2 \cdot \mathrm{cm}$. In order to keep the axial dimensions of the solenoid short, bucking coils were implemented (see Fig. 1) to reduce the stray flux at ~150 mm from the solenoid's center to the order of 10^{-4} T [5].

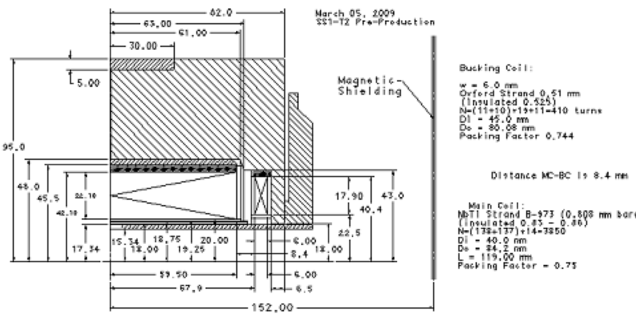

Fig. 1. HINS SS1-T2 pre-production solenoid design [4]

Due to the proximity to the SRF accelerators (see Fig. 2), the design requires a fringe field of less than 10 μT at a distance of 225 mm from the center of the solenoid. To achieve this, the solenoids are fitted with a 1-mm thick CRYOPERM-10 magnetic shield offering a relative permeability of 10,000 [2].

There are several locations in the solenoid's design of particular concern, where the magnetic shield is pierced. The design must allow for certain components to go through the shield in order to support or deliver cryogenics to the solenoid. This inevitably leads to field penetration near the beam tube, LHe pipes, support post, and alignment bars (see Fig. 8).

Manuscript received August 6, 2009. This work was supported in part by the U.S. Department of Energy, Office of Science.

Andrés G. Delannoy was with the University of Puerto Rico at Mayagüez, Mayagüez, PR 00681. This research was performed as part the SIST program with Fermi National Accelerator Laboratory (FNAL), P.O. Box 500, Batavia, IL, 60510 (e-mail: delannoy@fnal.gov).

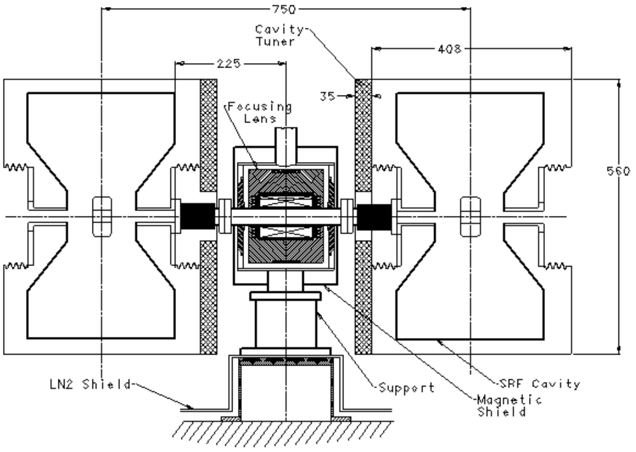

Fig. 2. Arrangement of HINS SS1 between two SRF cavities

The solenoid is expected to operate at a LHe temperature of 4.58 K once installed in the Meson Facility, instead of 4.2 K as anticipated in the original design. The design was modified (10% increase in main coil length) to compensate for the lower quench current and resulting decrease in current margin [4]. Given the expected quench current of around 190 A, the solenoid will generate a field of less than 7.2 T at its center.

III. Magnetic Measurement Method

The magnetic tests are intended to identify and address field strength and alignment concerns, among other complications [6]. The magnetic studies were carried out with a Hall probe array mounted on a copper plate, which contained eight Hall probes.

The probes were arranged perpendicular and parallel to the solenoid axis. This allowed the probes to quantify the radial and axial components of the magnetic field at a distance corresponding to where the plane of the SRF cavity wall will be.

The copper plate to which the Hall probes were mounted was cooled using liquid nitrogen. This helped minimize any thermal noise in the Hall probe signal. Two thermal straps allowed thermal contact between the plate and the liquid nitrogen vessel to maintain the plate at a temperature close to that of the LN_2.

A. Warm Measurements

Room temperatures measurements were performed in order to calibrate the magnetic measurement system and determine its ability to resolve the probe's signal from background noise. A 100-turn test coil was attached to each probe (see Fig. 3), which generated a weak field when driven by a given current. The probes were fixed to the center of the test coil, where the coil's transfer function could be easily determined.

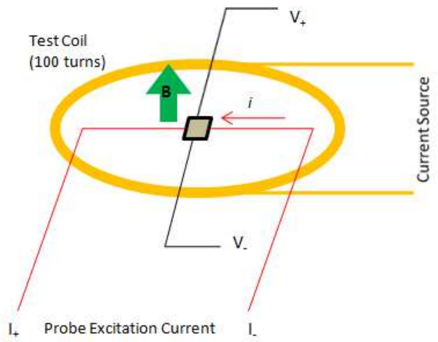

Fig. 3. Hall probe and test coil arrangement [6]. The probe was placed in the center of a 100-turn test coil.

Each probe's sensitivity was measured by driving a 30 mHz alternating current through each test coil. The voltage response of the corresponding Hall probe was recorded (see Fig. 4) while excited by a constant 100 mA. Since a linear correlation was expected between the current and the probe voltage [6], the output voltage vs. input current was plotted and a linear fit performed on it (see Fig. 5). The sensitivity was calculated by multiplying the slope from the linear fit (in mV/mA) times the tests coil transfer function (in mA/T) [6]. At this point, the test coil transfer function was assumed to have a constant value of 20 mA/G for all probes (see Table I).

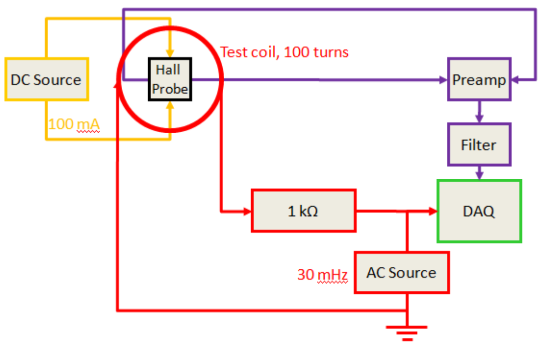

Fig. 4. DC probe excitation setup. The probe was excited by a constant 100 mA. The Hall probe signal was conditioned by a BJT preamp (x100 gain) and a low-pass filter. The test coil was driven at 30 mHz to simulate the solenoid's ramp profile. The 1 kΩ resistor allowed the current measurement.

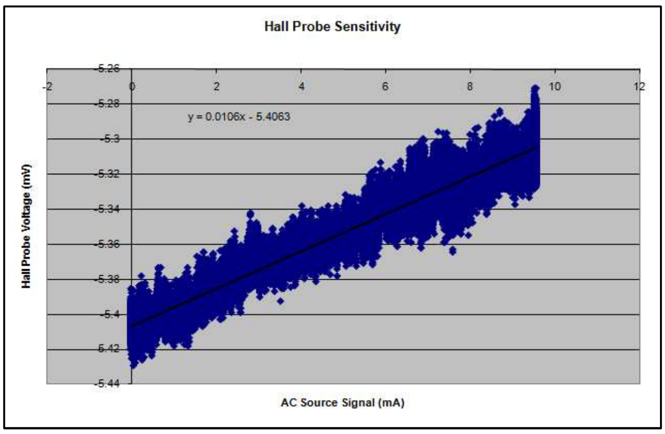

Fig. 5. Hall probe data correlation fit. This particular plot shows the behavior of probe no. 542 at 5 V_{AC}. This current corresponds to a magnetic field of around 0.24 G, generated by the test coil.

TABLE I
MEASURED AND MANUFACTURER RATED HALL PROBE SENSITIVITIES

Probe	Probe Number	Measured Probe Sensitivity (mV/T)	Manufacturer Probe Sensitivity Rating (mV/T)	Error %
1	542	20.56	40.3	48.98
2	543	20.86	36	42.05
3	541	45.07	61.8	27.08
4	546	20.35	45	54.78
5	545	11.30	24.2	53.29
6	544	21.84	28.7	23.92
7	540	19.06	31.5	39.49
8	539	26.56	34.9	23.89

The large amount of data points, data sets, and number of probes suggested the automation of data plots and calculations. A VBA excel macro was written to speed up the data analysis process. The user was expected to copy the entire data log to the clipboard, as recorded by a data gathering LabVIEW program: ‘hins1.vi’. When the VBA program was run, the data would be pasted, plotted, and analyzed automatically. This made hardware troubleshooting much faster and allowed the analysis of data while recording other probes. See the appendix for the commented VBA code.

After some investigation, it was concluded that the inconsistency in the measured and rated probe sensitivities was due to discrepancies in the Hall probe placement with respect to the test coil. As a consequence, the test coil’s transfer function could no longer be considered identical for each probe. The manufacturer’s rating for each Hall probe’s sensitivity was assumed correct and the transfer function was derived for each coil from the test data (see Table II).

TABLE II
TEST COIL TRANSFER FUNCTION PER COIL

Probe	Probe No.	Manufacturer Probe Sensitivity Rating (mV/T)	Test Coil Transfer Function (mA/G)
1	542	40.3	38.21
2	543	36	35.30
3	541	61.8	27.37
4	546	45	44.96
5	545	24.2	41.94
6	544	28.7	27.33
7	540	31.5	31.97
8	539	34.9	26.81

To determine the resolution of the Hall probes, the amplitude of the alternating current was decreased until the resulting magnetic field generated by the test coil was in the micro-Tesla range. The probe sensitivity was calculated for each decreasing AC test coil signal (see Fig. 6). The value of the sensitivity calculated at the highest current was considered the most accurate, and the remaining sensitivities were compared to this value.

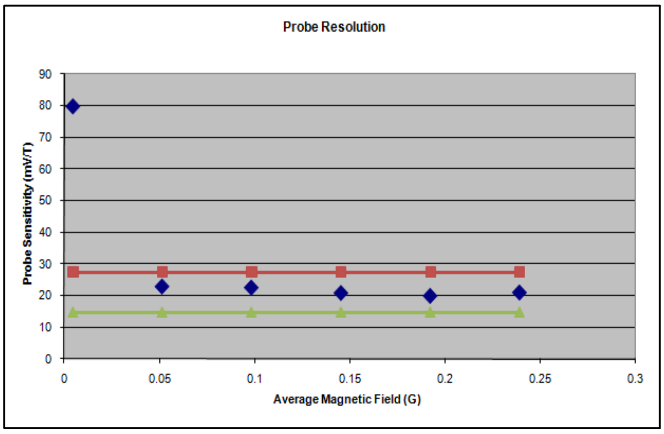

Fig. 6. Hall probe sensitivity measurement at varying magnetic fields. The plot shows data for probe no. 542. The red and green bars denote ±20% deviation from the sensitivity calculated at the highest field.

The measured data indicates that all probes can resolve the correct value of sensitivity at fields of 10 µT. As a general trend, the probes would resolve the correct sensitivity to within 20% accuracy at the 5 µT level.

B. *Cold Measurements*

The goal of cold measurements was to verify the solenoid performance in its operating conditions. The magnetic field generated by the solenoid is designed to undergo a five order-of-magnitude change across a distance of 225 mm. The design was modeled with simulation software to predict the solenoid’s stray field behavior (see Fig. 7). From the model analysis we should expected to measure a field of 6-8 µT at the distance corresponding to the cavity wall.

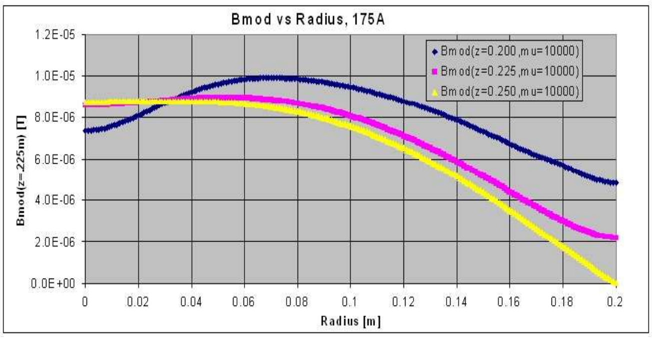

Fig. 7. Stray field behavior for HINS SS1 software model

A specific concern was whether the magnetic shielding was sufficient to maintain a stray magnetic field compliant with design constraints at a distance equivalent to the RF wall. Thus, the Hall probe array was arranged such that it would capture the magnetic field at this distance, after the solenoid’s magnetic field was attenuated by the bucking coils and CRYOPERM-10 shield (see Fig. 8).

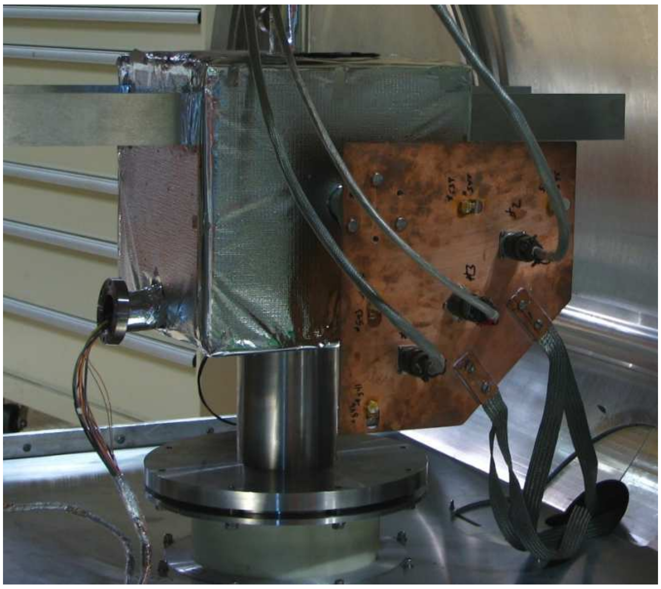

Fig. 8. Hall probe array installation. Note the magnetic shield box and alignment bars

A noise problem was encountered when driving the solenoid. The power supply was generating a ~500 μV level noise signal. This complication made recovering the Hall probe signal, which was at a ~100 μV level, very challenging. The situation was resolved by the introduction of a lock-in amplifier (see Fig. 9) to modulate the Hall probe excitation current and analyze its signal [6], in order to recover it from the noise.

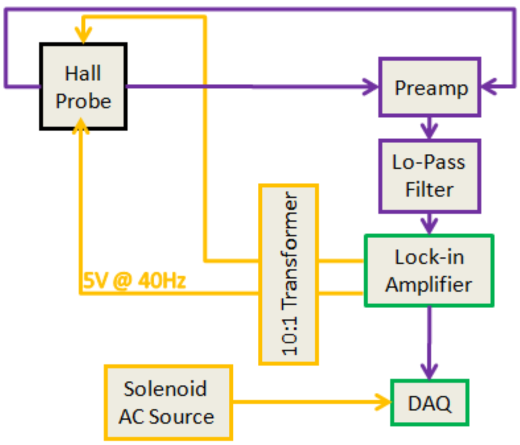

Fig. 9. Cold measurement setup. The data acquisition system recorded both lock-in amplifier channels and the solenoid's power supply signal. The lock-in amplifier drives the probe with 5 V_{AC} at 40 Hz, to avoid 60-cycle noise. The probe signal is amplified and conditioned before being processed by the lock-in amplifier.

The Hall probes' response to the solenoid field was captured (see Fig. 10) and compared to the power supply ramp profile. To simplify the analysis, the lock-in phase was adjusted in order for the X-channel to carry the Hall probe signal. The Y-channel only contained noise. This phase adjustment was stable for all probes, with minor corrections.

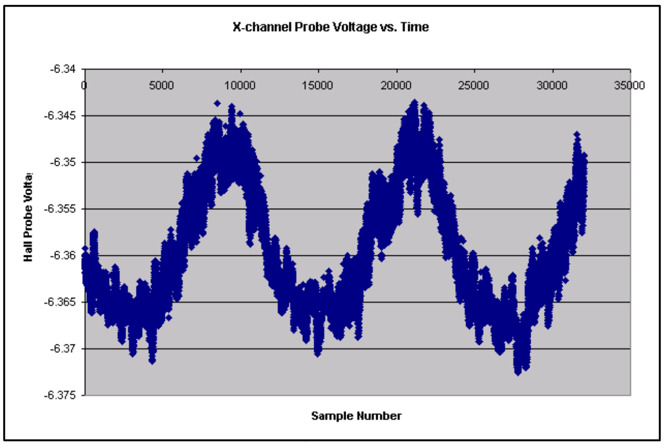

Fig. 10. X-channel probe signal as a function of time. The signal correlates considerably to the sinusoidal ramp profile used to drive the solenoid.

The test coil transfer function was also calculated for AC probe excitation and compared to the transfer function calculated for DC probe excitation. The values of the transfer function for each excitation method agreed within 5% for most probes (see Fig. 11). Further data is being taken to diagnose any discrepancies.

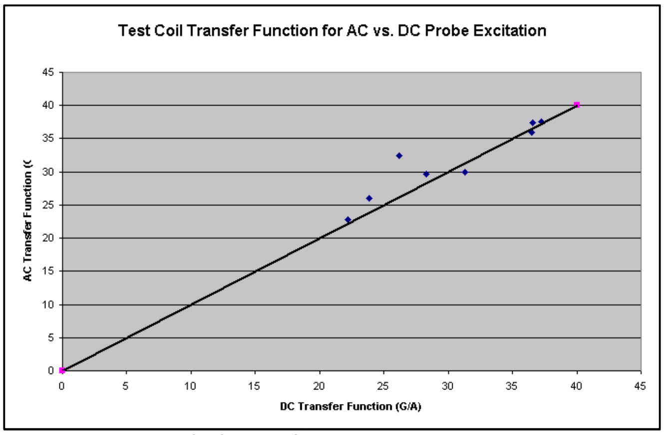

Fig. 11. Test coil transfer function for AC and DC probe excitation.

IV. Conclusion

The results obtained show that the Hall probe measurement system is capable of resolving magnetic fields almost an order of magnitude smaller than the required stray field at the location of the SRF cavity. It was shown that the idealized test coil transfer function for perfectly centered Hall probes is inaccurate. Instead, the transfer function was calculated for each probe assuming the manufacturer sensitivity ratings. These values are being studied more carefully using different probe excitation methods and conditions. Final and definitive results for the stray field of the solenoid at the distance of the SRF cavity are still pending more thorough calculations. At first glance, the data taken for the HINS SS1 solenoid design does seem to indicate that the current magnetic shield is sufficient to meet stray field requirements.

Appendix

VBA programs for excel were written by the author to automate warm measurement data plots and calculations. They are made available here: http://tinyurl.com/ACMacro-txt, http://tinyurl.com/DCMacro-txt.

A 3-D magnetic field recorder LabVIEW program was reviewed and modified in order to improve its functionality and usefulness. Documentation for '3AxisHallProbe.vi' is available made here: http://tinyurl.com/3DHallProbe-pdf

Acknowledgment

The author would like to thank Michael Tartaglia, Dmitri A. Sergatskov, the Magnet Systems Department, the HINS Magnet Group, and the SIST Committee for their assistance and guidance during this research.

References

[1] G. Chlachidze, et al., *HINS_SS1_SOL_02d Fabrication Summary and Test Results*, TD-09-001, FNAL, March 2009.

[2] G. Davis, M. Tartaglia, I. Terechkine, J. Tompkins, T. Wokas, *HINS Linac SS-1 Section Prototype Focusing Solenoid Design*, TD-08-010, FNAL, March 31, 2008.

[3] G. Davis, T. Page, M. Tartaglia, I. Terechkine, J. Tompkins, and T. Wokas, *HINS Linac SS2 Section Prototype Focusing Lens Design*, TD-09-003-1, FNAL, April 2009.

[4] G. Davis, T. Page, M. Tartaglia, I. Terechkine, J. Tompkins, and T. Wokas, *Pre-Production Solenoid for SS1 Section of HINS Linac*, TD-09-010, FNAL, April 2009.

[5] G. Davis, V.V. Kashikhin, T. Page, I. Terechkine, T. Wokas, *SS-1 Section Focusing Solenoid Prototype Cold Mass Design*, TD-06-041, FNAL, July 2006.

[6] A. Delannoy, *Weak Magnetic Field Measurement System*, FNAL, August 2008. Available: http://tinyurl.com/FNAL-Delannoy

[7] A. Judah, A. Delannoy, *Documentation for '3AxisHallProbe.vi'*, FNAL, July 2009. Available: http://tinyurl.com/3DHallProbe-pdf

[8] M. A. Tartaglia, et al., *Solenoid Focusing Lenses for the R&D Proton Linac at Fermilab*, PAC'09 (Fermilab-conf-09-143-TD), May 2009.

[9] R. C. Webber, et al., *Overview of the High Intensity Neutrino Source Linac*, Proceedings of LINAC08, Victoria, BC, Canada, MO301.